◇論 文◇

Physical and Electrochemical Properties of the Blended Cathode of $LiNi_{0.8}Mn_{0.1}Co_{0.1}O_2$ and $LiMn_{0.45}Fe_{0.55}PO_4/C$ for Lithium-ion Batteries

リチウムイオン電池用 $LiNi_{0.8}Mn_{0.1}Co_{0.1}O_2$ と $LiMn_{0.45}Fe_{0.55}PO_4/C$ 混合正極のキャラクタリゼーションと電気化学的特性

SHIOZAKI, Mayu； YAMASHITA, Hiroki*；
OGAMI, Takaaki**； KANAMURA, Kiyoshi***

塩 﨑 麻 由, 山 下 弘 樹*,
大 神 剛 章**, 金 村 聖 志***

ABSTRACT

Layered lithium nickel manganese cobalt oxide, $LiNi_{0.8}Mn_{0.1}Co_{0.1}O_2$ (NMC811) is one of the promising cathode materials for lithium-ion batteries due to its high energy density. This study investigated the electrochemical performances of blended cathodes of NMC811 and hydrothermally synthesized $LiMn_{0.45}Fe_{0.55}PO_4/C$ (LMFP) to improve cycling performance and rate capability of NMC811. At mixing ratios of 20 % or more LMFP, blended cathodes of NMC811 and LMFP showed the estimated 0.2C discharge capacities and energy densities by NMC811 and LMFP, whereas NMC811:LMFP=9:1 showed better 0.2C discharge capacities and energy densities than the estimated ones. The improvement in rate capability of NMC811 was particularly significant at LMFP mixing ratios of NMC811:LMFP = 8:2 or lower.

Keywords *: Lithium iron manganese phosphate, Lithium nickel manganese cobalt oxide, Blended cathode, Lithium-ion batteries*

＊中央研究所 資源・環境研究部 資源プロセスチーム
Processing for Resources Team, Mineral Resources & Environmental Research Department
＊＊中央研究所 資源・環境研究部 資源プロセスチーム リーダー
Manager, Processing for Resources Team, Mineral Resources & Environmental Research Department
＊＊＊東京都立大学 Tokyo Metropolitan University

要　　旨

高いエネルギー密度が得られる三元系$LiNi_{0.8}Mn_{0.1}Co_{0.1}O_2$（NMC811）はリチウムイオン電池の正極材料として注目されている．本検討では，NMC811の課題である容量維持率やレート特性を改善するため，これらの特性に優れる水熱法で合成したリン酸マンガン鉄リチウム$LiMn_{0.45}Fe_{0.55}PO_4$/C（LMFP）と混合して作製した正極の電気化学的特性の評価を行った．NMC811：LMFP=8:2以上のLMFPの混合比率ではNMC811およびLMFP単独の性能から推定される0.2C放電容量および質量エネルギー密度であったのに対し，NMC811:LMFP=9:1では推定値よりも優れた特性を示した．また，NMC811：LMFP=8:2以下のLMFPの混合比率において，特にレート特性の改善効果が大きかった．

キーワード：リン酸マンガン鉄リチウム，ニッケルコバルトマンガン酸リチウム，
混合正極，リチウムイオン二次電池

1. INTRODUCTION

Lithium-ion batteries are used in a variety of applications such as portable electronic devices, electric vehicles, and power storage facilities for solar and wind power generations. Especially for transportation applications, including electric vehicles, hybrid electric vehicles, and plug-in hybrid electric vehicles, lithium-ion batteries are recognized as one of the most suitable and promising energy-storage systems. In these applications, lithium-ion batteries are required to have high energy density, long lifetimes, and high thermal stability. In this respect, layered lithium nickel manganese cobalt oxide ($LiNi_xMn_yCo_zO_2$, generally referred to as NMC) is one of the most promising cathode materials due to its high energy density [1,2]. In particular, $LiNi_{0.8}Mn_{0.1}Co_{0.1}O_2$ (NMC811) has a high reversible capacity of nearly 200 mAh g^{-1} as reported before [3]. However, Ni-rich NMCs such as NMC811 are inferior in terms of capacity retention and thermal stability. As a solution to these problems, lithium manganese iron phosphate ($LiMn_{1-x}Fe_xPO_4$, LMFP) is one of the most promising cathode materials because of its extremely high thermal stability equivalent to $LiFePO_4$ (LFP) and excellent energy density superior to LFP [4]. In previous study, it was found that the thermal stability of NMC could be improved by blending LMFP with NMC [5]. Therefore, to achieve both a high energy density and a high thermal stability in lithium-ion batteries, the blended cathode of NMC811 and LMFP is considered a very promising approach. However, the effect of the blending ratio of NMC811 and LMFP on the physical characteristics, thermal stability and electrochemical performances (discharge capacity, rate capability, cycling performance, etc.) of the lithium-ion battery has not been fully investigated. Herein, of the two important characteristics of cathode materials, namely electrochemical performances and thermal stability, we study the electrochemical performances of the blended cathode of NMC811 and $LiMn_{0.45}Fe_{0.55}PO_4$/C at various blending ratios. In this study, we fabricate the blended cathodes with a practical level of high loading weight for high energy applications and assemble pouch cells to investigate their electrochemical performances.

2. EXPERIMENTAL

2.1 Cathode preparation

$LiNi_{0.8}Mn_{0.1}Co_{0.1}O_2$ (NMC811) was purchased from MSE Supplies LLC. $LiMn_{0.45}Fe_{0.55}PO_4$/C (LMFP) was synthesized by the hydrothermal method [6]. Composite cathode slurries using NMC811, LMFP, or a mixture of NMC811 and LMFP were fabricated by mixing 95.12 wt.% active material, 0.6 wt.% multi-walled carbon

nanotubes (Jiangsu Cnano Technology Ltd., LIB116-32) as the conducting agent, and 4 wt.% polyvinylidene difluoride (Solvay S.A., solef5130) as the binder in N-methyl-2-pyrrolidone (Wako Pure Chemical Ind. Ltd., special grade). The prepared slurry was coated on a carbon coated Al foil current collector (Shohoku Laminate Co., Ltd., thickness: 20 μm) using a doctor blade and dried at 80°C for 2 h in a vacuum oven. The loading weight of the cathode material on a carbon coated Al foil was approximately 10 mg cm^{-2} for NMC811, LMFP, and NMC811/LMFP cathodes. The composite cathodes with an area of 4.0 cm^2 (2.0 ×2.0 cm, 80-90 μm in thickness) were fabricated by roll-press.

2.2 Characterization

The crystalline phases of the samples were identified using powder X-ray diffraction (XRD) with a Bruker D8 Advance diffractometer with Cu Kα (λ = 0.15406 nm) radiation operating at 35 kV and 350 mA. The XRD patterns were collected in the 2θ range from 15 to 65° using a scanning step length of 0.0234° and scanning speed of 0.13 s/step. The particle morphologies of NMC and LMFP were observed using a field emission scanning electron microscope (FE-SEM, JSM-7001F) employing a secondary electron image detector and accelerating voltage of 15 kV. The average particle sizes of the samples were measured using the laser diffraction/scattering particle size distribution method with an MT3300EXII (MicrotracBEL Corp.) The specific surface areas of the samples were measured using the Brunauer–Emmett–Teller (BET) method with a FlowSorb III 2305 (Shimadzu Corp.) The electronic conductivities of the samples were measured using the powder resistivity measurement system MCP-PD51 (Nittoseiko Analytech Co., Ltd.) The true densities of the samples were measured with an MIC-1340-100cc (Shimadzu Corp).

2.3 Electrochemical measurements

The electrochemical properties of the fabricated cathodes were examined using pouch cells. Graphite electrode (Hohsen Corp., HS-LIB-N-Gr-001) was used as the anode. The electrolyte solution comprised 1.2 mol dm^{-3} $LiPF_6$ in a 3:7 mixture in volume of ethylene carbonate and ethyl methyl carbonate. 1 wt. % of vinylene carbonate and 0.5 wt.% of lithium bis(oxalato)borate were also added to the electrolyte. The separators comprised porous polyethylene (COD-20-B, W-Scope Corp.) The pouch cells were constructed in a drying chamber (dew point < −60°C).

The galvanostatic charge–discharge profiles and discharge rate capabilities were measured for the pouch cells at room temperature using a battery testing system (Hokuto Denko Corp., model: HJ1001SM8A). The charge behavior was tested in a voltage range of 2.5–4.2 V using a constant current constant voltage protocol at a current rate of 0.2C (34 mA g^{-1}). The discharge behavior was tested in a voltage range of 2.5–4.2 V using a constant current protocol at current rates of 0.2C (34 mA g^{-1}), 1C (170 mA g^{-1}), 3C (510 mA g^{-1}), and 5C (850 mA g^{-1}).

3. RESULTS AND DISCUSSION

3.1 Physical properties of NMC811 and LMFP

The XRD pattern of LMFP is shown in **Fig. 1**. The crystalline phase of LMFP was identified to be the $LiMn_{0.45}Fe_{0.55}PO_4$ olivine phase, and its crystal structure was assigned to the orthorhombic space group Pnma (No. 62) [7]. No impurities were detected in the XRD pattern.

The particle size and morphology of NMC811 and LMFP were observed using FE-SEM as shown in **Fig. 2**. The micron-sized secondary particles of

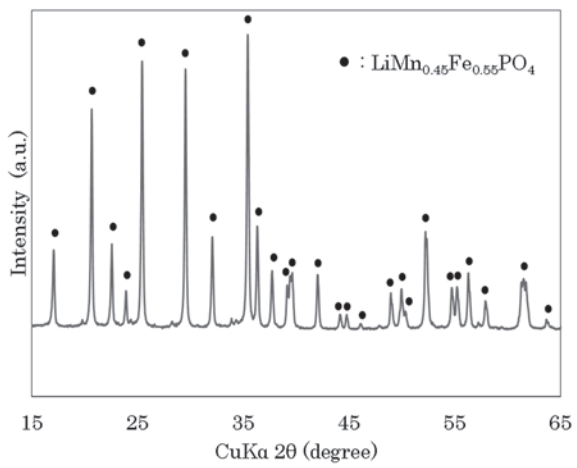

Fig. 1 XRD pattern of LMFP synthesized using the hydrothermal method

Table 1 Physical properties of NMC811 and LMFP

Sample	Electronic conductivity (S cm^{-1})	Specific surface area (m^2 g^{-1})	D_{50} (μm)	True density (g cm^{-3})
NMC811	3.32×10^{-2}	0.4	10.88	4.7
LMFP	6.97×10^{-6}	17.6	12.94	3.4

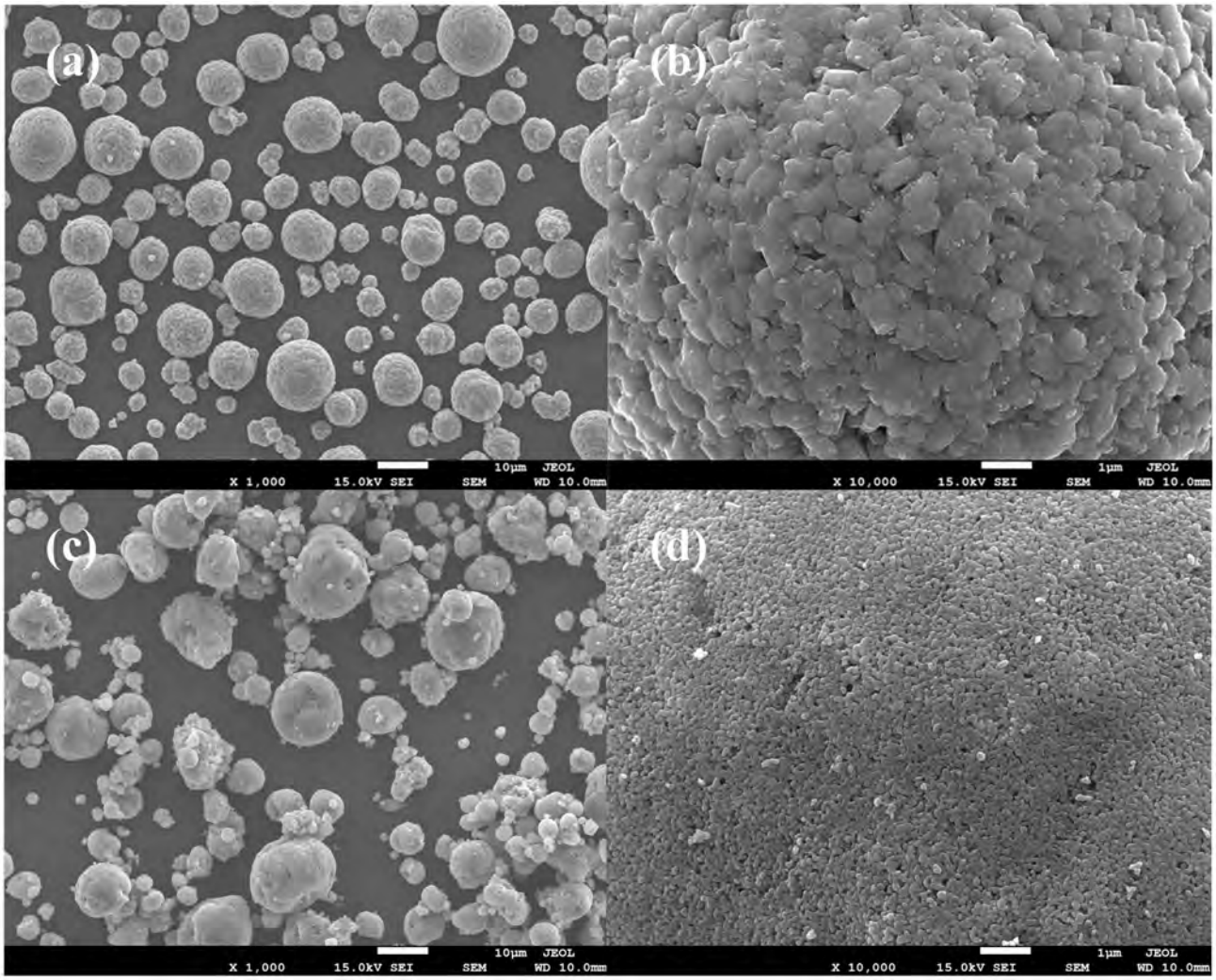

Fig. 2 SEM images of (a, b) NMC811 and (c, d) LMFP

NMC811 and LMFP comprising the nano-sized primary particles can be found in **Fig. 2(a)** and **(c)**. The secondary particles of LMFP were estimated to be slightly larger than those of NMC811. The secondary particles of both were around 10 μm in size and spherical in shape. The primary particles of NMC811 and LMFP are shown in **Fig. 2(b)** and **(d)**. The primary particles of LMFP were obviously much smaller than those of NMC811. The primary particle size of NMC811 was estimated to be around 1.0 μm, while that of LMFP was approximately 100 nm. The LMFP used in this study was synthesized by the hydrothermal method, which could be the reason for the uniform and small particles.

The physical properties of NMC811 and LMFP are shown in **Table 1**. The electronic conductivity of NMC811 was much higher than that of LMFP. The specific surface area of LMFP was much larger than that of NMC811, which was

Table 2 Loading weights, thicknesses, and densities of the cathodes of NMC811, LMFP, and NMC811/LMFP

LMFP ratio (wt.%)	Loading weight (mg cm^{-2})	Thickness (μm)	Density (g cm^{-3})
0	11.1	48	3.3
10	9.9	44	3.4
20	9.9	45	3.3
30	9.4	46	3.1
40	10.4	49	3.0
50	9.7	51	2.7
100	9.5	55	2.3

because the particles of LMFP were smaller than those of NMC811 as shown in **Fig. 2(b)** and **(d)**. The mean particle size (D_{50}) of NMC811 and LMFP was 10.88, and 12.94 μm, respectively. These results were consistent with their secondary particle sizes shown in **Fig. 2(a)** and **(c)**. The true density of NMC811 and LMFP was 4.7 and 3.4 g cm^{-3}, respectively. NMC811 was found to have a substantially higher true density compared to LMFP.

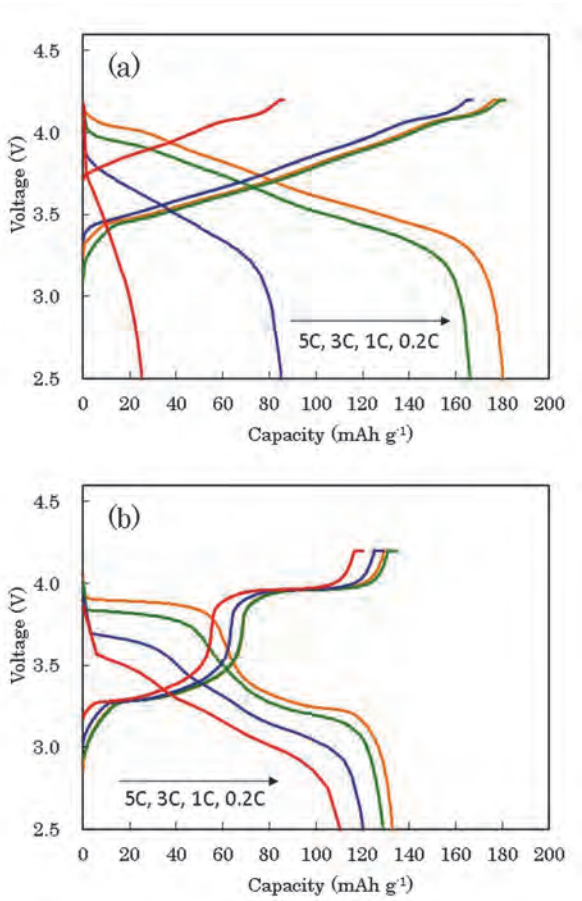

Fig. 3 Charge–discharge curves of (a) NMC811 and (b) LMFP

3.2 Electrochemical performance of NMC811 and LMFP

The cathodes of NMC811 and LMFP with a loading weight of approximately 10 mg cm^{-2} were fabricated. The assembled pouch cells with the NMC811 and LMFP cathodes were then charged/discharged within a voltage range of 2.5–4.2 V at a charge rate of 0.2C (34 mA g^{-1}) and at discharge rates of 0.2C (34 mA g^{-1}), 1C (170 mA g^{-1}), 3C (510 mA g^{-1}), and 5C (850 mA g^{-1}). The galvanostatic charge–discharge profiles of the cathodes are shown in **Fig. 3**. As shown in these profiles, NMC811 has no obvious plateaus in both charge and discharge curves, while LMFP has two distinct plateaus in both charge and discharge curves, respectively. The plateau around 3.2 V likely corresponds to Fe^{3+}/Fe^{2+} redox couple and the plateau around 4.0 V to Mn^{3+}/Mn^{2+} redox couple [8].

The discharge capacity of NMC811 was 180.1 mAh g^{-1} at 0.2C, 166.0 mAh g^{-1} at 1C, 85.0 mAh g^{-1} at 3C, and 25.2 mAh g^{-1} at 5C. The discharge capacity of LMFP was 132.8 mAh g^{-1} at 0.2C, 128.6 mAh g^{-1} at 1C, 120.2 mAh g^{-1} at 3C, and 110.3 mAh g^{-1} at 5C. The rate performance (5C/0.2C discharge capacity ratio) of NMC811 and LMFP was 0.14 and 0.83, respectively. LMFP has much higher rate performance than NMC811, while the

electronic conductivity of NMC811 is higher than that of LMFP (**Table 1**). Although the specific cause of this result needs to be identified, one possible cause can be that the cathode formulation used in this study is not optimal for NMC811.For instance, the amounts or ratios of carbon nanotubes and PVDF in the cathode formulation may be more optimized for NMC811.

The 0.2C gravimetric energy density of NMC811 and LMFP was 659 and 468 Wh kg^{-1}, respectively. NMC811 is known as a high energy density material, and its energy density is much higher than that of LMFP.

3.3 Electrochemical performance of the blended cathode of NMC811 and LMFP

We fabricated the blended cathodes of NMC811 and LMFP with blending ratios of NMC811:LMFP=9:1, 8:2, 7:3, 6:4, and 5:5. **Table 2** shows their main characteristics, including the loading weight which is approximately 10 mg cm^{-2}. As shown in **Table 2**, they all had similar loading weights and thicknesses. The density of the blended cathodes decreased with the increase in the ratio of LMFP. This was caused by the difference in the true density between NMC811 and LMFP as shown in **Table 1**.

The discharge capacities of the fabricated cathodes were measured using pouch cells. The results are shown in **Fig. 4**. In terms of the 0.2C discharge capacity, the blended cathode of NMC811:LMFP=9:1 showed a high discharge capacity (182.7 mAh g^{-1}) comparable to pristine NMC811 (180.1 mAh g^{-1}), in spite of the fact that LMFP had a lower discharge capacity than NMC811 (**Fig. 3**). At ratios of 20 wt.% LMFP and above, the discharge capacity gradually decreased. The 0.2C discharge capacity of the blended cathodes of NMC811:LMFP=8:2, 7:3, 6:4, and 5:5 was 169.9, 168.5, 163.5, and 156.2 mAh g^{-1}, respectively. The 0.2C discharge capacity of the NMC/LMFP blended cathodes as a function of the LMFP/(NMC+LMFP) weight ratio is shown in **Fig. 5**. The expected values were calculated by using the 0.2C discharge capacities of pristine NMC811 (180.1 mAh g^{-1}) and LMFP (132.8 mAh g^{-1}). For example, the expected 0.2C discharge capacity of NMC811:LMFP=9:1 was calculated as (180.1×0.9)+(132.8×0.1)=175.4. Comparison of the measured and expected values revealed that NMC811:LMFP=9:1 had a 0.2C discharge capacity higher than expected, indicating that its discharge capacity was equivalent to that of NMC811. At ratios of 20 wt.% LMFP or above, the measured discharge capacities were very close to the expected values. The cause of the higher-than-expected discharge capacity of NMC811:LMFP=9:1 remains unknown and requires more detailed analysis. One possible explanation for this phenomenon is that a small amount of LMFP does not block the electron pathway of NMC811, which has a higher electronic conductivity than LMFP, and thus does not interfere with the high electronic conductivity of the blended cathode of NMC811:LMFP=9:1. With the increase in the amount of LMFP in the blended cathode, the electron pathway of NMC811 may be blocked, possibly causing a decrease in the discharge capacity. The 0.2C gravimetric energy density of the blended cathodes showed the same tendency as the discharge capacity at the same current rate (**Fig.6**). The 0.2C gravimetric energy density of the blended cathodes of NMC811:LMFP=9:1, 8:2, 7:3, 6:4, and 5:5 was 667, 617, 611, 592, and 563 Wh kg^{-1}, respectively. NMC811:LMFP=9:1 had a high gravimetric energy density comparable to pristine NMC811, and at ratios of 20 wt.% LMFP and above, the energy density gradually decreased. Since the energy density is known to be affected by the discharge capacity of the cathodes, it is reasonable that they show coincidental tendencies.

The rate capability(fast discharge performance, defined here as 5C/0.2C discharge capacity retention) of the NMC811/LMFP blended cathodes as a function of the LMFP/(NMC+LMFP) weight ratio is shown in **Fig. 7**. The rate capability of the blended cathodes of NMC811:LMFP=9:1, 8:2, 7:3, 6:4, and 5:5 was 0.30, 0.37, 0.35, 0.38, and 0.44, respectively. The rate capability improved with the increase in the ratio of LMFP. This is because LMFP has a much higher rate capability than NMC811 as indicated in **Fig. 3**. However, the rate capability of the blended cathodes is not simply proportional to the LMFP/(NMC811+LMFP) weight ratio. The rate capability sharply improved at LMFP ratios of 20 wt.% and below, but the improvement was moderate with the LMFP ratio

increased to 30 wt.% or above. This tendency found in the rate capability appears to be slightly different from those of the 0.2C discharge capacity and energy density. As in the case of discharge capacity and e nergy density, the rate capability can be affected by the structure of the cathode. However, there may be some other factors that affect the rate capability. The definitive cause

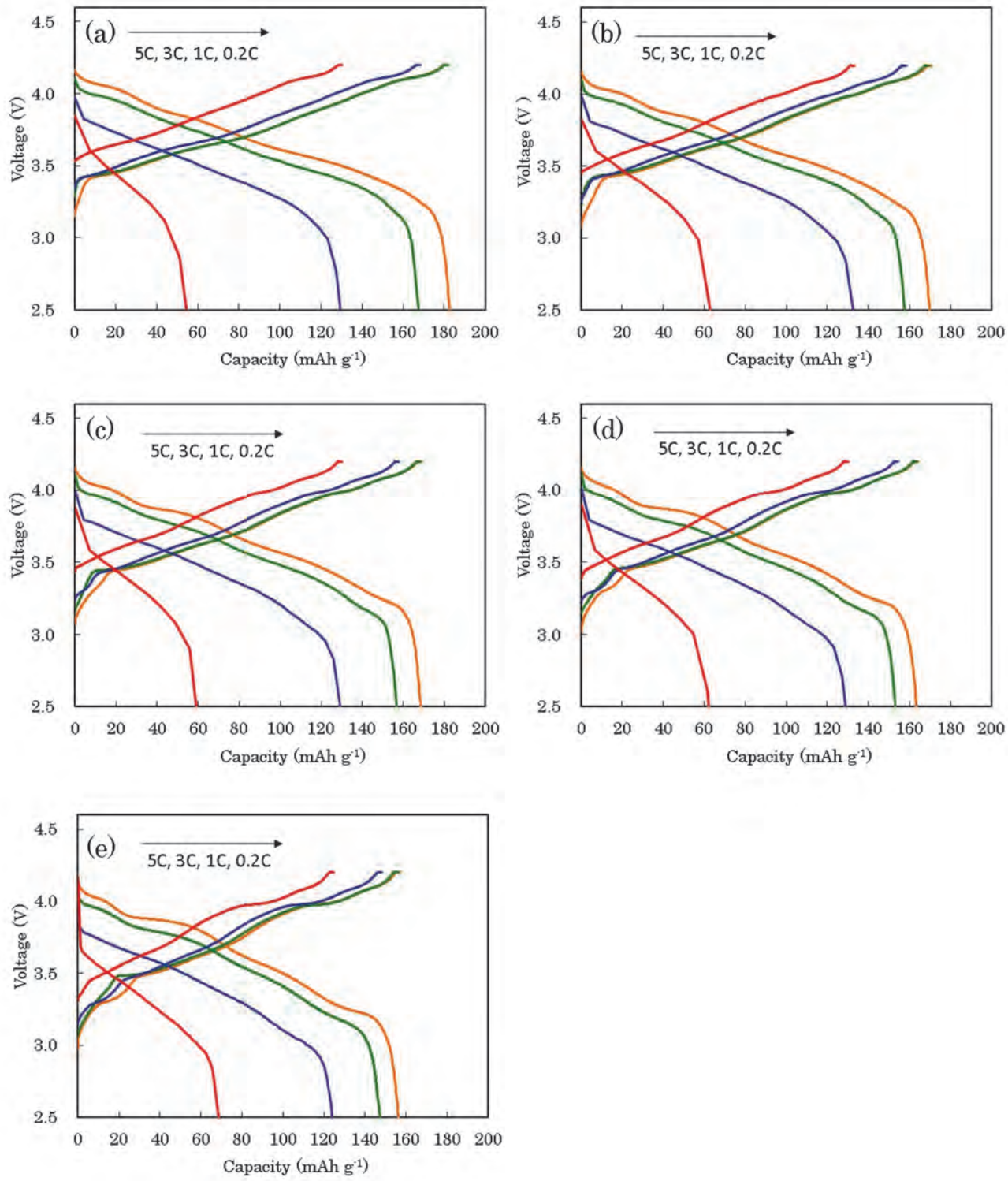

Fig. 4 Charge–discharge curves of blended cathodes at NMC811:LMFP = (a) 9:1, (b) 8:2, (c) 7:3, (d) 6:4, and (e) 5:5

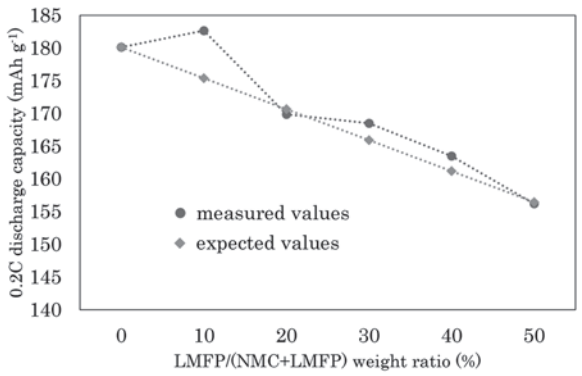

Fig. 5 0.2C discharge capacities of blended cathodes of NMC and LMFP as a function of LMFP/(NMC+LMFP) weight ratio in the cathode

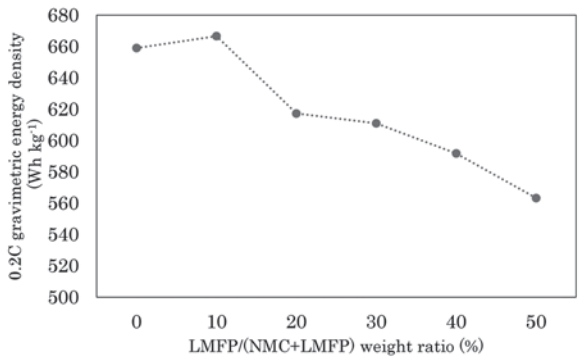

Fig. 6 0.2C gravimetric energy densities of blended cathodes of NMC and LMFP as a function of LMFP/(NMC+LMFP) weight ratio in the cathode

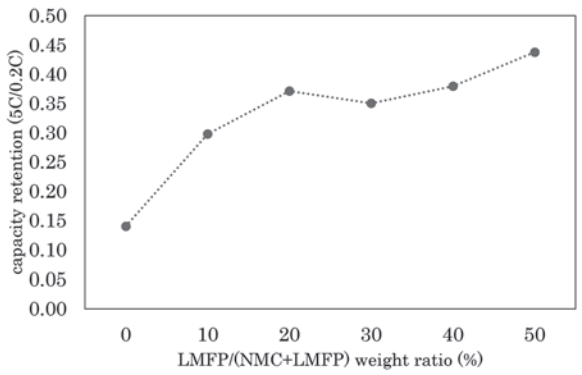

Fig. 7 Rate capabilities of blended cathodes of NMC and LMFP as a function of LMFP/(NMC+LMFP) weight ratio in the cathode

of the behavior of the rate capability remains unknown and requires more detailed analysis.

The tendencies of the discharge capacity, energy density and rate capability of the NMC811/LMFP blended cathode were revealed by this study. However, no analysis was made for the thermal stability of the blended cathode in this study. Research on this issue is very important because the use of NMC811 has been limited due to safety concerns associated with its low thermal stability. Previous study reported DSC results for pristine $LiMn_{0.8}Fe_{0.2}PO_4$, pristine $LiNi_{0.6}Mn_{0.2}Co_{0.2}O_2$, and a composite material of $LiNi_{0.6}Mn_{0.2}Co_{0.2}O_2$:$LiMn_{0.8}Fe_{0.2}PO_4$=7:3, in which the $LiNi_{0.6}Mn_{0.2}Co_{0.2}O_2$ / $LiMn_{0.8}Fe_{0.2}PO_4$ composite material exhibited a very similar exothermic peak to that of $LiMn_{0.8}Fe_{0.2}PO_4$ [5]. This result suggests that the thermal stability of $LiNi_{0.6}Mn_{0.2}Co_{0.2}O_2$ can be improved with the addition of $LiMn_{0.8}Fe_{0.2}PO_4$.

However, further research is needed to establish the optimal blending ratio of NMC and LMFP for ensuring both thermal stability and electrochemical performance.

4. CONCLUSIONS

This study investigated the effect of the blending ratio of $LiNi_{0.8}Mn_{0.1}Co_{0.1}O_2$ (NMC811) and $LiMn_{0.45}Fe_{0.55}PO_4$ (LMFP) on the physical and electrochemical performances of the blended cathode of NMC811 and LMFP for lithium-ion batteries. The cathode of NMC811:LMFP=9:1 showed high 0.2C discharge capacity and gravimetric energy density comparable to those of pristine NMC811. At ratios of 20, 30, 40, and 50 wt.% LMFP, the discharge capacity and energy density decreased with the increase in the ratio of LMFP. This was because NMC811 had higher discharge capacity and energy density than LMFP. In terms of the rate capability, the capacity retention (5C/ 0.2C) of NMC811 was much lower than that of LMFP. Although the exact cause needs to be identified, one possible explanation is that the cathode formulation used in this study may not be optimal for NMC811, presumably keeping the rate capability of NMC811 low. Because of the higher rate capability of LMFP than that of NMC811, the rate capability of the blended cathode improved with the increase in the

ratio of LMFP. However, its tendency was not simply proportional to the LMFP/(NMC811+LMFP) weight ratio. In addition, there was also a difference in the tendency between the discharge capacity and the rate capability which was a function of the LMFP/(NMC811+LMFP) weight ratio.

This study revealed that the blending ratio of NMC and LMFP had a very significant effect on the electrochemical performances of the NMC/LMFP blended cathodes. The electrochemical performances of the blended cathodes did not show a simple tendency, which suggested possible contributions of multiple factors. Further investigation is needed to determine the charge-discharge and energy storage mechanisms of the NMC/LMFP blended cathodes. Future research must also include detailed analysis on the thermal stability of the blended cathodes in order to solve the safety issues of the batteries.

REFERENCES

1) Kevin G. Gallagher; Steven Goebel; Thomas Greszler et al. Quantifying the promise of lithium–air batteries for electric vehicles. Energy & Environmental Science. 2014,7(5), p.1555-1563.
2) Dave Andre; Sung-Jin Kim; Peter Lamp et al. Future generations of cathode materials: an automotive industry perspective. Journal of Materials Chemistry A. 2015,3(13),p.6709-6732.
3) Hyung-Joo Noh; Sungjune Youn; Chong Seung Yoon et al. Comparison of the structural and electrochemical properties of layered $Li[Ni_xCo_yMn_z]O_2$ (x = 1/3, 0.5, 0.6, 0.7, 0.8 and 0.85) cathode material for lithium-ion batteries. Journal of Power Sources. 2013,233, p.121-130.
4) Surendra K. Martha; Judith Grinblat; Ortal Haik et al. $LiMn_{0.8}Fe_{0.2}PO_4$: An Advanced Cathode Material for Rechargeable Lithium Batteries. Angewandte Chemie International Edition. 2009,48(45),p.8559-8563.
5) Xiang Zhang; Mengyan Hou; Andebet Gedamu Tamirate et al. Carbon coated nano-sized $LiMn_{0.8}Fe_{0.2}PO_4$ porous microsphere cathode material for Li-ion batteries. Journal of Power Sources. 2020,448,e227438.
6) HIRAYAMA, Yuko; IKEGAMI, Jun; YAMASHITA, Hiroki et al. Electrochemical Performance and Thermal Stability of $LiMn_{1-x}Fe_xPO_4$/C (x=0.2,0.3,0.4) Secondary Particles. Journal of Research of the Taiheiyo Cement Corporation. 2019,177,p.41-52 (in Japanese).
7) Atsuo Yamada; Yoshihiro Kudo; Kuang-Yu Liu. Phase Diagram of $Li_x(Mn_yFe_{1-y})PO_4$ ($0\leq x, y\leq 1$). Journal of The Electrochemical Society. 2001,148(10),p.A1153-A1158.
8) Daniele Di Lecce; Jusef Hassoun. Lithium Transport Properties in $LiMn_{1-\alpha}Fe_\alpha PO_4$ Olivine Cathodes. The Journal of Physical Chemistry C. 2015,119(36),p.20855-20863.